

QUALITY ASSESSMENT OF OBJECT LOCATION AND POINT TRANSFER  
USING DIGITAL IMAGE CORRELATION TECHNIQUES

Wolfgang Förstner  
Photogrammetric Institute, Stuttgart University  
Germany, Federal Republic

Commission III

**Abstract:** The paper discusses aspects of evaluating the results of digital correlation used in photogrammetric high precision application. The most common correlation techniques are compared with respect to their optimization criteria. Results from practical and theoretical investigations concerning the sensitivity of the methods with respect to deviations of the mathematical model from reality are given. The aim of the paper is to provide some insight into the dependency of the main parameters of digital image correlation on the image texture, e.g. the pixel and the patch size, the quality of approximate values, the influence of unmodeled geometric distortions or of correlated noise. The results are useful for increasing the adaptability of the methods.

**Keywords:** Digital correlation, object location, point transfer, quality assessment, least squares, sensitivity, variance, convergency, pull-in range, geometric distortions, correlated noise, matched filter, Wiener Filter, phase correlation, robust estimators.

## 1. Introduction

1.1 Correlation techniques are widely used for relative and absolute measurements in time or space signals. Examples are electronic distance measurements based on the determination of phase differences, measurements of time delays in radio astronomy (very long base line interferometry), spectrum analysis in radar problems or speech analysis or parallax measurements in stereo vision systems. For more than 10 years automatic correlation techniques have been applied also in photogrammetry and remote sensing for the derivation of heights in stereo models for subsequent orthophoto projections or for registration and rectification of satellite images using ground control points. Hobrough in 1959 made the beginning with the instrumentation of parallax measurement for "Automatic Stereo Plotting". Since that time quite some systems have been developed. Most of them were designed for efficient generation of digital elevation models and/or differential rectification of aerial photos (e.g. Sharp et.al./IBM (1965), Hobrough/GPM (1971), Gambino and Crombie/CDC (1974), Helava/Bendix (1976), Hobrough/RASTAR (1978), Panton/CDC (1978), Marckwardt/Zeiss Jena (1982), cf. the review by Konecny and Pape (1981)).

1.2 Helava (1976) was the first to discuss the different aspects of digital correlation when it is realized in photogrammetric instruments, starting with an image model and using it for the evaluation of different parameters such as the pull-in range, the spot size and the optimum frequency, the effect of quantization etc.. He came to the conclusion that adaptability is a "problematic necessity: We know we need to adapt and we have the means but we have difficulties in deciding how and under what circumstances". High adaptability is realized e. g. by Hobrough (1971) for following the terrain roughness, by Widrow (1973) for matching chromosoms with the "rubber mask" technique, by Wong (1978) for changing the correlation threshold in different hierarchy levels or by Panton (1978) for keeping track with the changing perspective in two dimensional correlation. These examples show the efficiency of parameter tuning but also the necessity to start heuristically.

Of course the ability of adapting correlation parameters to the characteristic features of the object has to be seen in the context of the whole algorithm. This aspect has excellently been discussed by Makarovic (1980). It would be interesting to investigate how far his concepts are realized in non-photogrammetric applications of digital image processing especially in television image analysis, where image segmentation is more and more based on the estimation of the velocity

field and where the same algorithms are used for parallax estimation (cf. the extensive review given by Nagel (1981)).

1.3 Obviously these applications mainly aim at high performance rates rather than at high precision. Accuracies of one or a half pixel ( $\approx 10-50 \mu\text{m}$ ) seem to be good enough (cf. Dowman, 1982). In most cases the evaluation of the quality of a match is based on measures using different and unlinked types of mathematical models for the description of the algorithms and the image, such as the correlation coefficient, the slope of the correlation function or the difference of the grey levels of the images in concern. No information is used about the precision of the estimated location of the match in terms of a standard deviation. The situation is confirmed e. g. by the probably first application of digital image processing in high precision point determination with the "Automatic Reseau Measurement Equipment" (Roos/ETL, 1975), where with an extreme pixel size of  $0.8 \mu\text{m}$  empirical accuracies of  $1-1.5 \mu\text{m}$  are reached. This demonstrates the high technological standard of the system but also poses the question whether this precision could not have been reached with lower resolution (cf. Billingsley 1982).

Table 1 summarizes some of the available precision figures for object location and point transfer. They are given separately for empirical findings or estimations, for computer simulations and for values derived from theory. Except for the result of an epipolar line correlator (Claus, 1983)

Table 1 Precision of object location and point transfer (all figures in pels)

N <sup>o</sup>	Author	Year	Empirical	Simulations	Theoretical	Application/Remarks
1	Sharp et.al.	1965	1			DTM
2	v. Roessel	1972	2			DTM
3	Bernstein	1973 <sup>†</sup>	0.1			registration ( <sup>†</sup> cf.(1983))
4	Klaasman	1975			0.05	edge detection
5	Roos	1975	1-2			point determination
6	Cafforio/Rocca	1976	0.1			TV image sequences
7	McGille/Svedlow	1976			0.5/SNR	registration
8	Lichtenegger et.al.	1978	0.5			registration
9	Hill	1980		0.02-0.1		object location, binary images
10	Huang/Hsu	1981		0.02-0.1		parallax estimation
11	Wiesel	1981	0.1-0.3			registration
12	Bergmann	1982	0.5			TV image sequences
13	Förstner	1982			0.01-0.1	object location, point transfer
14	Thurgood/Mikhail	1982		0.02-0.1		target location
15	Ackermann/Pertl	1983	0.1-0.2			point transfer
16	Claus	1983	1.3			DTM, epipolar correlation
17	Ho	1983			0.02-0.2	object location, binary images
18	Mikhail	1983		< 0.05		target location

they refer to area matching procedures. There seems to be a tendency of the empirical results towards subpixel accuracy namely 0.1 pel or better, though already in 1973 Bernstein and independently in 1975 Cafforio and Rocca reached these figures. They seem to be realistically obtainable under production conditions and come very close to the coinciding results from computer simulations and theoretical developments. These, however, were not used for a thorough evaluation in photogrammetric applications until a few years ago.

This leads back to the fundamental problem of adaptivity, especially the question, under which conditions the accuracy inherent to the images can be used for object location and whether

the - compared to the theoretical values - low precision of some of the systems can be explained by theory.

1.4 The paper wants to discuss some of the aspects which are concerned with the quality assessment of digital correlation. It restricts to the dependencies of the different tunable parameters of the algorithms on the features of the correlated objects and thus in some way is complementary to Makarovic's paper (1980) which treats the systems aspect of correlation algorithms.

Section 2 first compiles and compares the most common matching procedures with respect to their optimality criteria. It turns out that they can be subdivided in two categories one optimizing the precision the other the reliability. The equivalence of the matched filter with the least squares estimator for the unknown location or parallax allows the combination of two well known mathematical tools, linear systems theory and adjustment theory which has first been realized by McGillem and Svedlow (1976). Thus one can take advantage of the experience of both fields of application, digital image processing and photogrammetry. Particularly interesting is the use of robust estimators and the extension of the procedures towards multiparameter estimators and multiimage correlation.

The quality in this context can be described by local, global and economic measures listed in table 2. The standard deviation of the estimated shift is the decisive measure for high precision application. As a criterion for the acceptance of a match it only has value if the result is

Table 2 Quality measures for digital correlation

N <sup>o</sup>	name	measure	type	causing effects
1	precision	standard deviation	local	random errors
2	sensitivity <sup>†</sup>	bias	local	systematic errors
3	convergency	pull-in range, rate of convergency	local, economic	approximate values
4	reliability <sup>†</sup>	probability of false match	global	approximate values
5	speed	calculation time	economic	algorithm
6	storage	compression rate	economic	coding

<sup>†</sup>the notion reliability in geodetic and photogrammetric literature means controllability and sensitivity, i.e. local properties of the estimators, thus it is differing from the notion above. This is because in those applications the signal to noise ration  $\sigma_s/\sigma_n$  is at least  $10^4$  and usually good approximate values are made available.

unsensitive to undetected or unmodelled systematic effects such as illumination or geometric distortion. On the other side the quality of the approximate values strongly influences the economy of a correlation algorithm. The convergency is also a local measure which might be described by the pull-in range or the rate of convergency. These three quality measures mainly depend on the texture of the object and are discussed in detail using a joint mathematical model. Section 3 also contains results on the reliability of correlation procedures and the effect of image coding onto precision and reliability. In contrast to the previous results they are based on computer simulations. The speed aspect is not treated as it highly depends on the optimization of whole algorithms which is determined by the specific area of application. The results of this section can be useful for increasing the adaptility of correlation algorithms.

Notation: Given  $g(x)$  with autocovariance function  $R_g(x) = g(x) * g(-x)$ . The inverse filter  $h(x)$  which yields  $\delta(x) = g(x) * h(x)$  is denoted by  $h(x) = g^{-1}(x)$ . Thus  $g^{-1}(x) * g(x) = g(x) * g^{-1}(x) = \delta(x)$ . It can be defined using the Fouriertransforms of  $g(x)$  and  $h(x)$ , namely  $G(u)$  and  $H(u)$  resp.:  $H(u) = 1/G(u)$  for all  $u$  with  $G(u) \neq 0$ , and  $H(u) = 0$  otherwise. Especially  $g^{-1}(x) = R_g^{-1}(x) * g(-x)$ .

We use this notation to avoid convolutions, especially deconvolutions in the spectral domain. This enables us to show clearly the shift of a function, which is a convolution with  $\delta(x-x_1)$ , instead of multiplying the spectrum with  $\exp(-j2\pi x x_1)$ . Substituting convolutions by matrix multiplications immediately yields the discrete formulas. In this case the inverse of a matrix has to be replaced by its pseudo inverse.

Stochastic variables, vectors or functions are underscored;  $\tilde{x}$  is the true value of the variable  $x$ .  $E(\cdot)$  and  $V(\cdot)$  denote the expectation and the variance operators. For notational convenience  $g(x)$  often is replaced by  $g$ . The signal to noise ratio (SNR) is defined by  $\sigma_g/\sigma_n$ .  $x'$  is the transposed vector of  $x$ .

2. Filters for Object Location and Point Transfer

2.1 Least squares filters

Let the template be given as a continuous greylevel function  $g(x)$ . According to fig. 1a the signal  $q_1(x)$  is observed which results from  $g(x)$  by

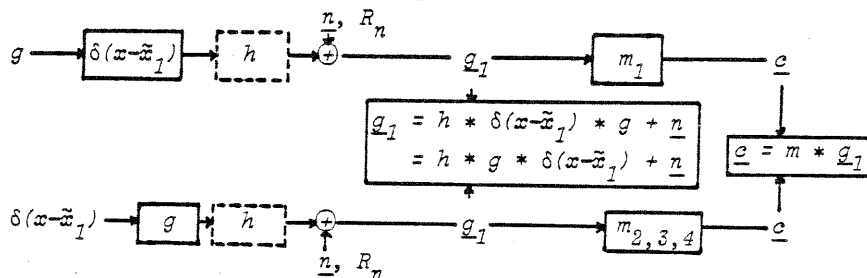
1. shifting the template by  $\tilde{x}_1$ , i.e. by convolving it with  $\delta(x-\tilde{x}_1)$
2. possibly convolving the result with the point spread function  $h(x)$  and
3. adding noise  $n(x)$  with autocovariance function  $R_n(x)$ ; thus

$$q_1(x) = h(x) * g(x) * \delta(x-\tilde{x}_1) + n(x) \tag{1}$$

It is assumed that  $g(x)$  and  $n(x)$  have zero mean.

Fig. 1 Object location: given  $g$ , possibly  $h$ ; observed  $q_1$ ; unknown  $\tilde{x}_1$ , noise  $n$

a.) matched filter for estimating  $\tilde{x}_1$



b.) filters for restoring  $\delta(x-\tilde{x}_1)$

In general  $n$  and  $\tilde{x}_1$  are unknown. The task is to find a filter  $m(x)$  such that the maximum of  $c(x) = m(x) * q_1(x)$ , the search function as we will call it, yields an estimate  $\hat{x}_1$  for  $\tilde{x}_1$ . We will compare the result of four different optimization criteria:

1.  $R_n$  known, maximize the signal to noise ratio of the filtered signal and the filtered noise at  $\tilde{x}_1$ :  $SNR^2 = V(g*m) / V(n*m)$ .
2.  $R_n$  known, maximize the ratio of the expected maximum and the average standard deviation of  $c(x)$  at all other points:  $R = E(q_1*m) / \sqrt{V(q_1*m)}$ .
3. The expectation of the search function should be a  $\delta$ -function with peak value at  $\tilde{x}_1$ :  $E(c(x)) \stackrel{!}{=} \delta(x-\tilde{x}_1)$ .
4. The maximum of  $E(c)$  should be at  $\tilde{x}_1$  and the autocovariance function of the search function should be a  $\delta$ -function:  $E(c(x)*c(-x)) = R_c(x) \stackrel{!}{=} \delta(x)$ .

The filter  $m(x)$ , the expectation of the search function and its autocovariance function are given in table 1 for the case where no filter  $h(x)$  is applied.

Table 1 Filters for Object Location

a.) Filter

N <sup>o</sup>	Name	Optimization Criterium	Filterfunction $m_i$
1	Matched Filter	$SNR^2 = V(\underline{g} * m) / V(\underline{n} * m)$ †)	$R_n^{-1} * g(-x) = R_n^{-1} * R_g * g^{-1}$
2	Wiener Filter for $\delta(x - \tilde{x}_1)$	$R = E(\underline{g}_1 * m) / \sqrt{E(\underline{g}_1 * m)}$	$R_{g_1}^{-1} * g(-x) = R_{g_1}^{-1} * R_g * g^{-1}$
3	Inverse Filter for $\delta(x - \tilde{x}_1)$	$E(\underline{e}(x)) \stackrel{!}{=} \delta(x - \tilde{x}_1)$	$R_g^{-1} * g(-x) = g^{-1}$
4	Phase Correlation	$R_e(x) \stackrel{!}{=} \delta(x)$	$(R_g * R_{g_1})^{-1/2} * g(-x) = R_{g_1}^{-1/2} * R_g^{1/2} * g^{-1}$

†) also least squares, maximum likelihood, best linear unbiased estimate (BLUE)

b.) Search function  $\underline{e}(x) = m(x) * \underline{g}_1(x)$  with  $\max(\underline{e}(x)) \Rightarrow \hat{x}_1$ 

N <sup>o</sup>	Name	Expectation $E(\underline{e}(x))$	Autocovariance function $R_e(x)$
1	Matched Filter	$R_n^{-1} * R_g * \delta(x - \tilde{x}_1)$	$R_n^{-2} * R_g * R_{g_1}$
2	Wiener Filter for $\delta(x - \tilde{x}_1)$	$(\delta - R_n^{-1} * R_n) * \delta(x - \tilde{x}_1)$	$R_g * R_{g_1}^{-1}$
3	Inverse Filter for $\delta(x - \tilde{x}_1)$	$\delta(x - \tilde{x}_1)$	$R_g^{-1} * R_{g_1}$
4	Phase Correlation	$R_g^{1/2} * R_{g_1}^{-1/2} * \delta(x - \tilde{x}_1)$	$\delta$

Discussion:

1. The first filter  $m_1 = R_n^{-1} * g(-x)$  is the most commonly used *matched filter* (for a derivation see e.g. Castleman 1979, p. 210). In case  $\underline{n}$  is white noise, i. e.  $R_n$  is a  $\delta$ -function, the expectation of the search function  $\underline{e}_1$  is the autocovariance function  $R_g(x - \tilde{x}_1)$  of the template shifted by the unknown value  $\tilde{x}_1$ . It is well known that this filter is also optimal in the least squares sense, where the difference  $\int (g - g_1)^2 dx$  between  $g$  and  $g_1$  is minimized (Svedlow et al. 1976, McGillem and Svedlow 1977, Meyers and Franks 1980, Ryan et al. 1980). Furthermore  $m_1$  also yields the best linear unbiased estimator (BLUE) for the unknown shift, i. e. it leads to the smallest variance in this class of estimators (McGillem and Svedlow 1977). Finally  $\hat{x}_1$  is also the maximum likelihood estimator if the noise can be assumed to be normally distributed (McGillem and Svedlow 1976). The cited equivalencies are generally valid for least squares solutions (cf. e.g. Koch 1980).

In view of these overpowering criteria there seems to be no chance to find better filters. Actually at least three others exist. The reason for their development was the experience that the matched filter in practice often leads to unreliable results namely to mismatches at very wrong positions. This is due to the local character of the optimization criteria. All three filters try to minimize the probability of a false match by sharpening the searchfunction.

2. The second filter  $m_2 = (R_g + R_n)^{-1} * g^{-1} * R_g$  explicitly tries to optimally separate between the true position  $\tilde{x}_1$  and all others (Emmert and McGillem 1973). The main part of the search function is a  $\delta$ -function. As  $\underline{g}_1$  can also be generated by convolution of the now unknown function  $\delta(x - \tilde{x}_1)$  with the given filter  $g(x)$  and subsequent degradation with  $\underline{n}(x)$  (cf. fig. 1b) the filter  $m_2$  actually is identical with the *Wiener Filter* for restoring the function  $\delta(x - \tilde{x}_1)$ .

3. The third filter  $m_3 = g^{-1}$  is the *inverse filter* neglecting the influence of the noise. The average search function is a  $\delta$ -function located at the correct position. This filter seems to be superior to the preceding. But generally this is not true. Though both filters  $m_2$  and  $m_3$  are highpassfilters (for normal imagery) the transfer function  $M_2(u)$  of  $m_2$  is bounded if the signal to noise ratio  $\sqrt{P_g(u)/P_n(u)}$  is not going to infinity, which seems to be a realistic assumption, whereas  $M_3(u)$  might have poles namely if  $G(u)$  has zeros.

4. The covariance functions  $R_{\underline{c}_2}$  and  $R_{\underline{c}_3}$  show that both filters prefer one of the both functions  $g$  or  $\underline{g}_1$ . The fourth filter  $m_4 = (R_g * R_{g_1})^{-1/2} * g(-x) = (m_2 * m_3)^{1/2}$  is a compromise namely the geometric mean of the filters  $m_2$  and  $m_3$ . The search function  $\underline{c}_4(x) = (R_g * R_{g_1})^{-1/2} * g(-x) * \underline{g}_1(x)$  is fully symmetric with respect to the given functions  $g$  and  $\underline{g}_1$ . The covariance function  $R_{\underline{c}_4}$  is a  $\delta$ -function. The Fouriertransform  $\underline{C}_4(u) = G^* \underline{G}_1 / |G^* \underline{G}_1|$  of  $\underline{c}_4$  contains only the phase of the crosspower spectrum  $G^* \underline{G}_1$  of  $g$  and  $\underline{g}_1$ . This filter  $m_4$  is therefore called the *phase correlation filter* (Kuglin, Hines, 1975; Pearson, Hines, Golosman, Kuglin, 1977). The formulas given by Pratt already 1974 are a discrete version of  $\underline{c}_4(x)$  and are motivated by prewhitening both functions  $\bar{g} = R_g^{-1/2} * g$ ,  $\bar{\underline{g}}_1 = R_{g_1}^{-1/2} * \underline{g}_1$  and then correlating  $\bar{g}$  and  $\bar{\underline{g}}_1$ . The phase correlation method thus treats all frequencies of the crosspower spectrum with the same weight leading to results which are very robust to narrow banded distortions or long waved disturbances. The pictures given by Oppenheim (1981) demonstrate that the phase of the amplitude spectrum really contains the main part of the geometric information of an image.

5. A comparison of the autocorrelation functions  $R_{\underline{c}}$  of the search function  $\underline{c}(x)$  reveals that in case the signal to noise ratio is large the three filters  $m_2$ ,  $m_3$  and  $m_4$  lead to similar results; in the noise free case they are identical. On the other side if the noise component in  $\underline{g}_1$  is large one needs a good estimate or a priori knowledge about the covariance function  $R_n$ , except when using the phase correlation technique, which does not need any a priori information about  $n$ . The matched filter  $m_1$  obviously is most sensitive to assumptions concerning the noise as, in contrary to  $m_2$  and  $m_3$ , errors in  $R_n$  and thus in  $R_{g_1}$  do not compensate but cumulate. This is the price to be paid for obtaining the locally best solution. In case  $R_n$  and  $R_g$  are proportional, i. e.  $R_g = \text{const.} \cdot R_n$  all four filters are identical. This situation realistically can be assumed if images are contaminated not only by film grain noise but also by long waved distortions, either geometric or time dependent ones (cf. Emmert and McGillem 1973, Svedlow and McGillem 1976), but also is met in radar signals where this type of filter is well known (cf. Urkowitz, 1953).

6. The filters can also be used in a slightly modified form when in addition to the noise and the shift the template is passed through a linear filter  $h(x)$  before being observed, which might represent smearing effects caused by the atmospheric turbulence or the movement of the sensor. Then  $\underline{g}_1 = h * g * \delta(x - \tilde{x}_1) + n$  and thus  $R_{g_1} = R_n * R_g + R_n$  with  $R_h = h(x) * h(-x)$ . Then all filters have to be modified by substituting  $g$  by  $g * h$ , e. g. now the second filter reads as  $m_2 = (R_g * R_n + R_n)^{-1} * g(-x) * h(-x)$ . As the filter  $h(x)$  usually is not known precisely one uses a symmetric surrogate  $\bar{h}(x) = \bar{h}(-x)$ . But then  $\underline{c}_1$  only is unbiased if the true function  $h(x)$  also is symmetric. Otherwise, e. g. in case of onesided illumination effects, systematic errors have to be expected, as e. g.  $E(\underline{c}_1(x)) = R_n^{-1} * R_g * \bar{h}^{-1} * h * \delta(x - \tilde{x}_1)$  does not have its maximum value at  $x = \tilde{x}_1$ , because  $\bar{h}^{-1} * h$  is not symmetric with respect to  $x = 0$ . The bias  $E(\underline{c}_1) - \tilde{x}_1$  in addition to  $\bar{h}$  depends on  $R_g$  and  $R_n$ .

7. The optimality and the linearity of the filters  $m_1$ ,  $m_2$  and  $m_4$  is only given for known correlation function  $R_n$  thus known  $R_{g_1}$ . If  $R_n$  or  $R_{g_1}$  is estimated from  $\underline{g}_1$  e.g. by cyclic correlation or what is equivalent by taking the inverse Fourier transform of the empirical cross power spectrum, the analysis of the properties of the search function becomes much more involved as the filters are not linear anymore. This especially holds for the phase correlation technique the way it was originally formulated by Kuglin and Hines (1975). On the other side, Emmert and McGillem (1973) and Pratt (1974) proposed to approximate the autocovariance function, namely by assuming an autoregressive image model (cf. section 3.1). A similar adaption leading to a nonlinear filter is the common standardization of the cross covariance function  $g(-x) * \underline{g}_1(x)$  leading to the cross correlation function  $\underline{c}(x) = g(-x) * \underline{g}_1(x) / \sqrt{R_g(o) \cdot \hat{R}_{g_1}(o)}$  where an estimate  $\hat{R}_{g_1}(o) = \hat{R}_{g_1}(o)$  is used for the variance of the signal  $\underline{g}_1$ . Cross correlation not only is invariant to unknown brightness differences of  $g$  and  $\underline{g}_1$  but in its discrete and local version is highly adaptive to varying illumination.

Summarizing one may distinguish two types of filters for object location:

- a. The filters  $m_2$ ,  $m_3$  and  $m_4$  are restoration filters for the unknown function  $\delta(x-\tilde{x}_1)$ . The phase correlation filter  $m_4$  is the geometric mean of the inverse filter  $m_3$  and the Wiener Filter  $m_2$ . It is invariant to arbitrary prefilters  $h(x)$  which degrade the object  $g(x)$  and robust with respect to bandlimited or longwaved distortions, such as oscillations, clouds, reseau crosses, shadows, temporal changes, local geometric distortions etc. Assuming usual imagery all three filters are high pass filters. They minimize the probability for a false match, which however seems not to be proved rigorously up to now. Though they do not yield optimum precision, i. e. the smallest possible standard deviation for the estimated shift, they are very well suited for determining good approximate values  $\hat{x}_1$  for  $\tilde{x}_1$  in extreme cases (cf. Emmert and McGillem 1973, Pratt 1974) even down to signal noise ratios below 1 (Ehlers 1983).
- b. The matched filter  $m_1$  leading to optimal precision has only local properties and is therefore suited for high precision application, provided the mathematical model (geometric, radiometric, stochastic) is adequate. As the model eq.(1) is oversimplified and only suitable for detecting the location of one object in one image we will next discuss other optimization functions and extensions of the matched filter.

## 2.2 Robust filters

1. The equivalence of the least squares and the maximum likelihood estimator for normally distributed noise suggests to base the estimation on other, especially longtailed distributions. This leads us to robust estimators. Here the maximum likelihood type estimators seem to be best suited as they fit quite well into classical least squares algorithms. Such estimators are obtained by instead of minimizing the sum of squares one minimizes the sum of less increasing functions  $\rho(v_i)$  of the residuals  $v_i$ :  $\sum_i \rho(v_i, x) \rightarrow \min.$ , e.g.:

$$\underline{c}(x) = \sum_i \rho(g_1(x_i) - g(x_i - x)) \rightarrow \min. \quad (2)$$

Robust estimators can easily be realized using a least squares algorithm by modifying weights or residuals after each iteration step (cf. Huber (1981), p. 181 ff): thus one either minimizes  $\sum v_i^2 p_i$  with  $p_i = \rho(v_i)/(v^2 + k^2)$  (with  $k^2 \ll \sigma^2$ , cf. Krarup et al. 1980) or minimizes  $\sum \bar{v}_i^2$  with  $\bar{v}_i = \sqrt{\rho(v_i)}$ . The approach using modified residuals is most attractive as the set up of the normal equation matrix needs not to be changed.

2. Several choices of the function  $\rho(v)$  are proposed (cf. Huber (1981), Götze (1983), Kubik (1984)):

- a. The choice  $\rho(v) = v^2/2$  leads to the classical least squares solution being a special case of
- b. The choice  $\rho(v) = |v|^p$  leads to the minimization of the  $L_p$ -norm. The well known least sum technique going back to Laplace results from taking  $p = 1$ . Using this method, however is not optimal, as large disturbances still have an influence on the estimator (cf. Förstner and Klein (1984) and Werner (1984). Other functions have been proposed by Hampel, Andrews or Tukey which eliminate this effect.

Also the exponential function

- c.  $\rho(v) = v^2/2 \cdot \exp(-v^2/2)$  proposed by Krarup et. al. (1980) and known as the Danish method guarantees that large discrepancies do not influence the result.

3. The least sum method is the most commonly applied robust method, as it is the fastest one (cf. Gambino and Crombie 1974). It is used e.g. by Barnea and Silverman (1972), Limb and Murphy (1975), Wong and Hall (1979) for template matching. Widrow (1973) has used the method for his

rubber mask technique. The corresponding estimate for the standard deviation the median absolute deviation (MAD) has been applied by Bailey et. al. (1976), whose results however do not go quite conform with the expectation, because using the MAD as optimization criterium only is superior to the covariance maximization when the signal to noise ratio is high. Martin and McGath (1974) have applied robust techniques for detecting signals in noise assuming the probability density function of the noise to be a mixture of Gaussian density functions. Their limiter-quadratic detector belongs to class c. where large discrepancies do not influence the results. (cf. also Kuznetsov 1976)

4. The impact of robust estimators on template matching lies in the fact that during line following the influence of unpredictable disturbances (clouds, reseau-crosses, shadows) onto the unknown parameters can be totally eliminated, not only partly reduced as when using the phase correlation technique. Hence, these disturbances need not be treated with methods of pattern recognition unless they are robustified themselves. This also holds for cases where parts of the object are hidden by another one. Here the residuals, i. e. the gray level differences will be large enough to be weighted down thus having no impact onto the estimated shift. This allows to reach the segmentation borders without too much loss in accuracy.

### 2.3 Extensions of the matched filter

In this section we want to discuss several modifications and extensions of the matched filter which are already in use or could be used to advantage in standard applications of photogrammetry and remote sensing.

1. The most important application of the filters for object location is their use for *point transfer*. This seems to be trivial but in view of the optimality criteria it is not. The model for point transfer is

$$\begin{aligned} g_1 &= g * \delta(x - \tilde{x}_1) + n_1 \\ g_2 &= g * \delta(x - \tilde{x}_2) + n_2 \end{aligned} \quad (3)$$

where now the shifts  $\tilde{x}_1$  and  $\tilde{x}_2$ , the noises  $n_1$  and  $n_2$  but also the template  $g$  are unknown. The task is to estimate the unknown shift difference  $\tilde{x}_{12} = \tilde{x}_2 - \tilde{x}_1$ . It is easy to rewrite eq. (3) into a form very similar to eq. (1) using the estimates  $\hat{\tilde{x}}_{12}$ ,  $\hat{n}_2$  and  $\hat{g} = \overline{(g_1 - n_1)}$ :

$$g_2 = \hat{g} * \delta(x - \hat{\tilde{x}}_{12}) + \hat{n}_2 \quad (4a)$$

But now the difference becomes apparent: The optimization of object location assumes the object to be deterministic whereas point transfer, using an estimate  $\hat{g}$  as template, has to cope with an object having stochastical properties. Of course the filters derived for object location can be applied here substituting  $g_1 \rightarrow g_2$  and  $g \rightarrow \hat{g}$ . But then at least  $g$  has to be restored, estimated from  $g_1$  (or  $g_2$  or both) making some assumptions about  $R_n$  and  $R_g$ , using a Wiener filter and solving eq. (4) for  $\tilde{x}_{12}$  while keeping  $\hat{g}$  fixed. Of course this is an approximation. A rigorous solution still has to be found.

2. Object location and point transfer in two dimensional images or sequences cannot be restricted to estimating shifts. The images usually are more or less distorted radiometrically or geometrically (cf. e.g. Bernstein and Ferneyhough 1974). Though one could think also of correlating three dimensional objects we will restrict the discussion to the two dimensional case. Here eq. (1) should be generalized to

$$g_1(x, y) = T_r \{ g [ T_g(x, y; p_g) ] + n(x, y); p_r \} \quad (5)$$



where  $T_r(g; p_r)$  and  $T_g(x, y; p_g)$  stand for arbitrary radiometric or geometric transformations which depend on the parameter vectors  $p_r$  and  $p_g$ . We thus reach the problem of *multiparameter estimation*.  $T_r$  and  $T_g$  might e.g. be linear transformations.  $T_r$  then compensates for contrast and brightness and  $T_g$  for differential perspective, i.e. affine distortions, neglecting the local curvature of the terrain (cf. Pertl 1984):

$$\begin{aligned} T_r(g) &= a_1 g + a_2 \\ T_g(x, y) &= \begin{pmatrix} T_{gx}(x, y) \\ T_{gy}(x, y) \end{pmatrix} = \begin{pmatrix} b_1 & b_2 \\ b_4 & b_5 \end{pmatrix} \begin{pmatrix} x \\ y \end{pmatrix} + \begin{pmatrix} b_3 \\ b_6 \end{pmatrix} \end{aligned} \quad (6)$$

Other parameters could describe nonlinear transformations or e. g. the width of the point spread function  $h(x)$  (cf. Thurgood and Mikhail 1982).

Of course the additional parameters have to be predicted using a priori information or estimated from the available data. The necessity to compensate for scale and rotation, possibly affinity and the inability of the classical matched filter to provide an estimate lead to more or less sophisticated prediction schemes (cf. eg. Hobrough (1971), Kreiling (1973) or Panton (1978)). Direct solutions are given by Emmert and McGillem (1973) for affinity parameters and by Casasent and Psaltis (1976) for scale and rotation. They used invariance properties of the amplitude spectrum. In general estimating two or more parameters requires a refined searching strategy to reduce the numerical effort. Hill-climbing or gradient methods for estimating additional parameters are widely used and discussed in section 3.2 (cf. e.g. Schalkoff and McVey 1979, Wild 1979, Huang and Tsai 1980, Meyers and Frank 1980, Förstner 1982, Thurgood and Mikhail 1982).

3. The idea of deriving parameters from the amplitude spectrum, which is invariant to shifts, suggests to look for algorithms which do not extract the information from the gray levels directly but derive the shifts or other parameters from *functions of the gray levels*.

The most promising approach is to use invariants of the images. Thus instead of comparing  $g$  and  $g_1$  one compares  $I(g)$  and  $I(g_1)$ , where  $I$  is a function invariant to transformations  $T_r \in C_r$  out of a class  $C_r$  of expected gray level transformations:  $I[g(x)] = I[T_r[g(x)]]$ . Similarly one could use functions which are invariant to an expected class of geometric transformations.

Using the *gradient* or *edge image* is the most commonly method being invariant to a large class of temporal gray level changes of the image (cf. Hobrough 1959, Anuta 1970, Wong 1978, Makarovic 1980, Wiesel 1981). As taking the derivative of an image is high pass filtering this yields a sharper peak in the correlation function (cf. Pratt 1974). It can therefore be a surrogate for one of the filters  $m_2$ ,  $m_3$  or  $m_4$  for obtaining a  $\delta$ -like correlation function. The precision of the estimated shift however is not increased by this means (cf. Anuta 1970 and sect. 3.3.1).

Other functions which are used for correlation are *invariant moments* (cf. Wong and Hall 1978) and *Hadamard coefficients* (v. Roessel 1972). The concept of *Fourier descriptors* commonly used in the field of pattern recognition seems to be very powerful for object location as the identification and the location process are performed simultaneously within the same mathematical framework besides being invariant to scale and rotation of the image in concern (cf. Wallace and Mitchell 1980, Mikhail et al. 1983) The proposal of Masry (1981) to correlate *entities*, i.e. features extracted from the image, seems to be a quite general concept as not only objects with closed boundary can be handled (cf. Lugnani, 1982).

Quite differently motivated image functions are the complex exponentiation (Göpfert 1977) and the binary or polarity correlation (cf. Makarovic 1980, Marckwardt 1982). The *complex exponentiation*  $T_r(g(x)) = \exp(-jp \cdot g(x))$ , with  $p$  depending on the variance of  $g$ , aims at whitening the signal. Though this is not valid in general, e. g. for a rectangular function, the correlation function  $T_r(g) * T_r(g_1(-x))$  for normal imagery yields a much sharper peak than the cross correlation. This

method is one of the fastest gray level transformations approximation a high pass filter if one uses table-look-up procedures (cf. Ehlers 1983). *Binary* or *polarity correlation* on the other side aims at high speed, but usually leads to relatively poor results though the autocorrelation function due to the arcsin-law (cf. Papoulis 1965, p.484) is sharp peaked (cf. the broad discussion by Helava 1976). Binary correlation should therefore only be used for determining approximate values or in cases where ultimate precision is not demanded.

The modifications discussed up to now have frequently been applied and have made algorithms more flexible and reliable when being confronted with varying types of templates. The method of template matching however has to be embedded into more general tasks such as aerial triangulation deformation measurements or mosaiking where not only one channel or one pair of images are to be handled.

4. *Multi-image object location* occurs when several satellite images are simultaneously registered on the basis of well defined ground control points. The corresponding model is described by eq. (3); but now the template  $g$  is given. The task is to identify the same object in two or more images. The algorithmic solution reduces to simple object location only if the degrading noises  $\underline{n}_1$  and  $\underline{n}_2$  are uncorrelated. If however they have common terms, the estimation process for the two shifts has to take into account the correlation. It might be caused by stochastic or deterministic effects such as unmodelled geometric distortions or unknown filters  $\tilde{h}_1(x)$  and  $\tilde{h}_2(x)$  the object is passed through.

5. More involving is the simultaneous relative rectification of three or more images using *multi-image correlation*. Eq. (3) then has to be complemented by one or more further equations, e.g.  $\underline{g}_3 = g * \delta(x - \tilde{x}_1) + \underline{n}_3$ . Now again  $g$  is unknown. The relative shifts  $\tilde{x}_{12} = \tilde{x}_2 - \tilde{x}_1$ ,  $\tilde{x}_{23} = \tilde{x}_3 - \tilde{x}_2$  and  $\tilde{x}_{31} = \tilde{x}_1 - \tilde{x}_3$  have to be determined. Obviously only two of them are independently estimable. This gives rise to a condition equation  $\tilde{x}_{12} + \tilde{x}_{23} + \tilde{x}_{31} = 0$  for the estimated shift differences. It can be introduced into the estimation process (cf. Ackermann 1982) or it might at least serve as a triangle check for detecting false correlations which proves to be very effective (Tanaka et. al. 1978, Ackermann and Pertl 1982).

6. No severe problems causes the simultaneous correlation of several channels of an MSS or colour image at least from the theoretical point of view. The *multi-channel correlation* can also be described by eq. (1) but now  $g$ ,  $\underline{g}_1$  and  $\underline{n}$  are vectors depending on  $x$ . Thus with e. g. two channels  $a$  and  $b$  one has to solve

$$\begin{aligned} \underline{g}_{1a}(x_i) &= g_a * \delta(x_i - \tilde{x}_1) + \underline{n}_a(x_i) \\ \underline{g}_{1b}(x_i) &= g_b * \delta(x_i - \tilde{x}_1) + \underline{n}_b(x_i) \end{aligned} \quad i = 1, \dots \quad (7)$$

for  $\tilde{x}_1$ , which is the discrete version of the estimation problem. Observe that we now have two templates  $g_a$  and  $g_b$ , only one unknown shift. Collecting the corresponding vectors in one vector, e.g.  $g' = (g'_a, g'_b)$ , allows to rewrite eq. (7) and to obtain the discrete version of eq. (1):  $\underline{g}_1(x_i) = g' * \delta(x_i - \tilde{x}_1) + \underline{n}$ . The matched filter obviously requires the covariance matrices  $C_{n_a n_a}$  and  $C_{n_b n_b}$  but also  $C_{n_a n_b}$ . If the noise vectors  $(\underline{n}_a(x_i))$  and  $(\underline{n}_b(x_i))$  are uncorrelated the shift can be separately estimated from both channels. The estimates then have to be averaged using their standard deviation (cf. sec. 3.2). Whereas film grain or electronic noise of different channels in MSS or colour images will not be correlated correlations between  $\underline{n}_a$  and  $\underline{n}_b$  might result from unmodelled geometric distortions.

Experiences by Anuta (1970) seem to prove that different channels of MSS images contain different geometric information, thus a combined estimation should lead to better results than estimations from single channels. On the other hand the investigations of Prabhu and Netravali (1982) show that the luminance component of colour images is sufficient for the prediction

necessary for data compression in image sequences. This suggests that only parts of the spectral information are necessary for precise template matching.

Further research will show which spectral bands are decisive for high precision object location and which impact multiimage correlation has on the precision and reliability of point transfer.

### 3. Quality of Digital Image Correlation

This section presents several quality measures which can be used for the assessment of digital image correlation. They are based on the matching algorithms presented in the previous section especially on the least squares approach and on proper image models. The aim is to provide some insight into the relations between the algorithm, the geometric model and the texture of the template in order to visualize the limitations of the quality measures but also their value for increasing the flexibility and the reliability of the procedures.

#### 3.1 Image models

The prediction of correlation quality has to be based on an adequate image model. In this context the image gray level function  $g_1(x)$  usually is assumed to form a stochastic process consisting of the true image  $g(x)$  and additive noise  $n(x)$ :  $g_1(x) = g(x) + n(x)$ , where  $g$  and  $n$  are mutually uncorrelated stationary processes. If one further assumes them to be Gaussian the covariance functions  $R_g$  and  $R_n$  or the power spectra  $P_g$  and  $P_n$  being their Fourier transforms fully describe their statistical properties.

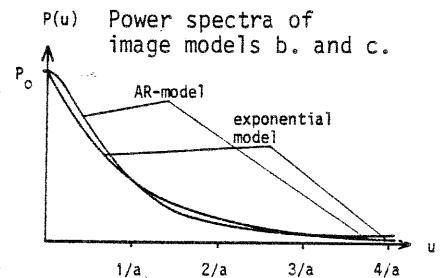
There are three main types of processes in use to describe  $g$  and  $n$  (cf. table 4):

- The white noise model is only used to describe  $n$ .
- The exponential model is proposed by Helava (1976) to describe  $g$  and is based on extensive empirical investigations. Its parameters  $P_0$  and  $a$  are measures for the brightness and the contrast of the image. A value of  $a = 0.2 \text{ mm}$  belongs to good imagery.
- The autoregressive model (AR-model) is used very frequently in digital image processing (cf. Rocca 1972, Pratt 1974, Emmert and McGillem 1973, Rosenfeld 1976). Also here  $P_0$  and  $r$  describe the brightness and the contrast. This model sometimes also is used to describe correlated noise (cf. sect. 3).

Table 4 Image and noise models

N <sup>o</sup>	name	$R(x)$	$P(u)$
a	white noise	$\sigma^2 \delta(x)$	$\sigma^2$
b	exponential model	$R_0 / (1 + (2\pi x/a)^2)$	$P_0 e^{-a u }$
c	autoregressive model	$R_0 e^{- x /r}$	$P_0 / (1 + (2\pi ru)^2)$

Fig. 2



The difference between models b. and c. (cf. fig. 2) seems to be negligible. We can relate the models e. g. by assuming both power spectra to have the same values at 0 and  $1/a$ . This leads to the relation  $r = \sqrt{e-1} / 2\pi a \approx a/5$ . The variance of the estimated shift however depends on the effective bandwidth  $b$  of the signal which for white noise does not exist for the AR-image model.

$b$  can be determined from

$$b^2 = \frac{\int u^2 P_g/P_n \, du}{\int P_g/P_n \, du} = \begin{cases} 2/a^2, & \text{1-dimensional signal} \\ 3/a^2, & \text{2-dimensional signal} \end{cases} \quad (8)$$

For the AR-image model and white noise the integral in the numerator is infinite. For the expo-

nential image model with white noise the effective bandwidth is  $\sqrt{2}/a$  and  $\sqrt{3}/a$  for one dimensional and two dimensional isotropic signals.  $b$  can be interpreted as the standard deviation of the frequency having the standardized  $SNR^2(u)$  as probability density function.

The parameter  $\sigma$  can be estimated from the empirical autocovariance function. The variance of the noise can directly be measured if one uses flat imagery with no structure. The variation of  $g$  then reflects the (film grain) noise (cf. Helava 1976, Ryan 1980). But  $P_g(0)$  and  $\sigma_n^2$  can rigorously estimated using variance component estimation techniques (cf. Koch 1980) which for digital terrain profiles has given realistic results (cf. Lindlohr).

### 3.2 Precision of object location

We will now derive formulas for determining the variance of the estimated shifts after object location. We start with the discrete two-dimensional model

$$g_1(x_i, y_i) = g(x_i - \hat{x}, y_i - \hat{y}) + n(x_i, y_i), \quad i = 1, \dots, n \quad (9)$$

This equation holds for all  $n$  pixels which need not form a grid.

The idea is to linearize eq. (9) and solve the linearized problem using least squares technique (cf. Limb and Murphy 1975, Burckhardt and Moll 1978, Wild 1979, Meyers and Frank 1980, Thurgood and Mikhail 1982). Hence since nearly 10 years this method has been applied for image sequence analysis (Cafforio and Rocca 1976, Schalkoff and McVey 1978, Fennema and Thompson 1979, Dinse et. al. 1981, Huang 1981) and recently for target location and point transfer in photogrammetry and remote sensing (Ackermann and Pertl 1982, Förstner 1982, Mikhail 1982).

Starting from approximate values  $x_0$  and  $y_0$  and setting  $\Delta g_i = \Delta g(x_i, y_i) = g_1(x_i, y_i) - g(x_i - x_0, y_i - y_0)$  and  $v_i = v(x_i, y_i) = n(x_i, y_i)$  the unknown differences  $\hat{x}$  and  $\hat{y}$  (assuming  $x_0 = y_0 = 0$  for the moment) can be estimated from the  $n$  equations

$$\Delta g_i + v_i = g_{x,i} \hat{x} + g_{y,i} \hat{y} \quad i = 1, \dots, n \quad (10)$$

where  $g_x = \partial g / \partial x$  and  $g_y = \partial g / \partial y$  are taken at the approximate values. The overdetermined equation system (10) leads to the normal equations

$$\begin{pmatrix} \Sigma g_x^2 & \Sigma g_x g_y \\ \Sigma g_x g_y & \Sigma g_y^2 \end{pmatrix} \begin{pmatrix} \hat{x} \\ \hat{y} \end{pmatrix} = \begin{pmatrix} \Sigma g_x \Delta g \\ \Sigma g_y \Delta g \end{pmatrix} \quad (11a)$$

if the disturbing noise is white,  $\sigma_n^2 = 1$ . It can be rewritten if the sums are replaced by the corresponding variances or covariances, e.g.  $\Sigma g_x g_y = n \sigma_{g_x g_y}$

$$n \begin{pmatrix} \sigma_{g_x}^2 & \sigma_{g_x g_y} \\ \sigma_{g_x g_y} & \sigma_{g_y}^2 \end{pmatrix} \begin{pmatrix} \hat{x} \\ \hat{y} \end{pmatrix} = n \begin{pmatrix} \sigma_{g_x \Delta g} \\ \sigma_{g_y \Delta g} \end{pmatrix} \text{ or } N \cdot \underline{x} = \underline{h} \quad (11b)$$

Eq. (11) yields optimal estimators for the unknown shifts. Their covariance matrix for general  $\sigma_n^2$  is

$$C_{zz} = \begin{pmatrix} \sigma_x^2 & \sigma_{xy} \\ \sigma_{xy} & \sigma_y^2 \end{pmatrix} = \frac{\sigma_n^2}{n} \begin{pmatrix} \sigma_{g_x}^2 & \sigma_{g_x g_y} \\ \sigma_{g_x g_y} & \sigma_{g_y}^2 \end{pmatrix}^{-1} \quad (12)$$

1. The precision of the location is determined by three parameters

- the image noise variance
- the number of pixels and
- the variance and the covariance of the gradient image. This is a specification of the edge business in an image which proves to be decisive for the precision of object location.

If the image is isotropic, i.e. the covariance of the gradients is zero we obtain the variances

for  $\hat{x}$  and  $\hat{y}$  separately, e.g. (cf. Förstner 1982)

$$\sigma_x^2 = \frac{1}{n} \frac{\sigma_n^2}{\sigma_{g_x}^2} = \frac{1}{n} \frac{1}{SNR^2} \frac{\sigma_g^2}{\sigma_{g_x}^2} = \frac{1}{n} \frac{1}{SNR^2} \frac{1}{(2\pi b_x)^2} \quad (13)$$

with the signal to noise ratio  $SNR = \sigma_g / \sigma_n$  and the effective bandwidth  $b_x = \sigma_{g_x} / (2\pi\sigma_g)$  in x-direction (cf. McGilllem and Svedlow 1976, Ryan et.al. 1980). Svedlov et. al. (1976) have given the continuous form of eq. (13) omitting the number of pixels and assuming the template and the noise to follow the same model, i.e.  $P_g/P_n = const.$ . Eq. (13) also is the Cramer-Rao bound giving a lower bound for the variance when using an arbitrary filter (cf. Ryan et. al. 1980, Meyers and Frank 1980). Moreover the variance  $\sigma_{g_x}^2$  of the gradient is identical to the curvature of the autocorrelation function due to the moment theorem  $\sigma_{g_x}^2 = -P_{xxx, g}(0)$  (cf. Papoulis 1965, p. 317; Ryan et.al. 1980). This specifies the criteria used by Helava (1976) or Panton (1978) namely the "drop" or the "slope" of the autocorrelation function.

On the other side the normal equations might be singular. This situation occurs when one wants to correlate straight edges. One may use the pseudo inverse of  $N$  in this case, but the estimated shifts then are not unbiased any more. Thus only the part of the shift orthogonal to the edge is determinable which shows up in a very flat error ellipse for the estimated location.

2. Assuming the exponential image model together with white noise one now can derive a simple relation for the standard deviation

$$\begin{aligned} \text{1-dimensional: } \sigma_x &= \frac{1}{2\pi\sqrt{2}} \frac{1}{\sqrt{n}} \frac{\alpha}{SNR} \\ \text{2-dimensional: } \sigma_x &= \frac{1}{2\pi\sqrt{3}} \frac{1}{\sqrt{n}} \frac{\alpha}{SNR} \end{aligned} \quad (14)$$

The standard deviations for point transfer are larger by a factor  $\sqrt{2}$ , if the noise in both images has the same variance (cf. Förstner 1982).

The results of computer simulations by Huang and Hsu (1981) are in full agreement with the theoretical predictions (cf. fig 3 and 4). The linear dependency of the variance on the number of pixels, i.e. the block size, is clearly visible, as doubling the length of the block size decreases the variance by a factor 4. Already with the 16 x 16 block a standard deviation of 0.1 pel is reached, proving the least squares algorithm to yield subpixel accuracy.

Fig. 3 Variance of estimated shift in [pels<sup>2</sup>] vs. the number of pixels (block size); computer simulations by Huang and Hsu (1981)

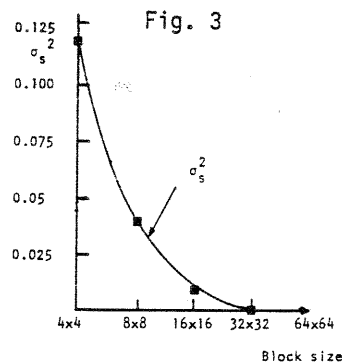


Fig. 4 Standard deviation in [pels] of estimated shift vs.  $\sigma_n$ ; computer simulations by Huang and Hsu (1981), block size 9x9

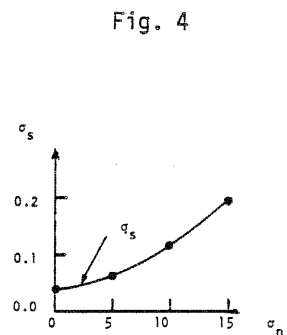


Fig.4 demonstrates the effect of additional noise when using a block size of 9 x 9. The case with  $\sigma_n=0$  shows that at least some noise is inherent to the procedure possibly due to discretization errors. This might explain the deviation of the result from a straight line as it would be expected from theory.

### 3.3 The effect of filters onto the precision

If another filter than the matched filter is used for object location the variance of the estimated shift will be larger. This might occur if one uses one of the filters for sharpening the peak of the correlation function or if the noise is actually coloured and one applies the matched filter assuming the white noise model. For simplicity we will restrict the discussion to the one-dimensional case.

1. The template and the signal are assumed to be passed through a filter  $h$ , e.g. yielding  $\bar{g} = h * g = H g$  with  $H$  for the moment being the circulant matrix with kernel vector  $h$  cf. Rosenfeld, Kak 1976). Assuming the noise to be white the least squares solution for  $\hat{x}$  from  $\Delta g_i + \bar{v}_i = \bar{g}_{x,i}$  with uncorrelated error equations is not optimal. It leads to the estimator

$$\begin{aligned} \hat{x} &= (\bar{g}'_x \bar{g}_x)^{-1} \bar{g}'_x \Delta g \\ &= (g'_x H' H g_x)^{-1} g'_x H' H \Delta g \end{aligned} \quad (15)$$

Using the covariance matrix  $C_{\Delta g \Delta g} = C_{nn}$  we obtain the variance of  $\hat{x}$  from error propagation

$$\sigma_x^2 = g'_x H' H C_{nn} H' H g_x \cdot (g'_x H' H g_x)^{-2} \quad (16)$$

If we choose  $h$  such that  $H' H = C_{nn}^{-1} = \sigma_n^{-2} I$  then eq. (16) reduces to eq. (13). In order to be able to use the exponential image model we have to transform eq. (16) into continuous form and then apply Parseval's identity (cf. McGillem and Svedlov 1976, Förstner 1982). We obtain

$$\sigma_x^2 = \frac{1}{4\pi^2 n} \frac{\int u^2 P_g P_n P_h^2 \hat{c}u}{[\int u^2 P_g P_h \hat{c}u]^2} \quad (17)$$

where  $P_h$  is the power spectrum of the now continuous filter  $h$ . We discuss two important cases.

a. The commonly used transformation  $T_x(g(x)) = dg(x)/dx$  yields the gradient image and may represent edge images (cf. sect. 2.3).  $T_x$  is a linear filter with transferfunction  $H(u) = -j2\pi u$  (not to be mixed up with the matrix  $H$  above), thus with power spectrum  $P_h = 4\pi^2 u^2$ . Working out the integrals we obtain the variance of the shift  $\sigma_x^2(T_x(g)) = 5/4 \cdot \sigma_n^2 \cdot a^3 / (4\pi^2 n)$ . Compared to the variance  $\sigma_x^2(g(x)) = 1/2 \cdot \sigma_n^2 \cdot a^3 / (4\pi^2 n)$ , which one would reach with the optimal matched filter, correlating the gradient signals leads to a standard deviation which is a factor 1.6 higher. This proves that sharpening the peak of the correlation function in order to improve the reliability does not increase the precision (cf. the experimental results by Anuta (1970)).

b. An ideal low pass filter with upper frequency  $u_o$  can be used to approximate sampling with a pixel size of  $\Delta x_o = 1/2u_o$ . According to Förstner (1982) there exists an optimal frequency if the number of pixels and the signal to noise ratio is kept fixed, namely  $u_{oo} = 3.38 / a$ , where  $a$  is the parameter describing the sharpness of the image. For good aerial photos with  $a = 200 \mu m$  this leads to an optimum pixel size of  $\Delta x_{oo} = 30 \mu m$ , which seems to be realistic. On the other side if one keeps the length  $d = n \Delta x$  of the object fixed oversampling does not change, namely deteriorate the precision as long as a good approximation for  $g_x$  is used (if necessary) and all frequencies  $u < u_{oo}$  are represented. As the powerspectrum  $P_{g_x}(u)$  of the gradient has its maximum at  $2/a$ , one should at least use the band around this frequency (cf. Helava 1976), which is  $10 \text{ lp/mm}$  for good imagery.

The influence of the median filter is discussed below.

c. Eq. (16) can also be used to get an idea how reliable the estimated variance  $\sigma_x^2$  is if we incorrectly assume the noise to be white when in reality it is coloured. For this we substitute  $H' H$  by the inverse  $C^{-1}$  of the covariance matrix actually used in the estimation process. We can now study the effect of different covariances  $C$  onto the variance  $\sigma_x^2$ . The choice  $C = C_{nn}$  yields the

least squares variance. If we now specify  $C_{nn}$  and assume the noise to follow the AR-model then  $C_{nn}$  is a Toeplitz matrix  $C_{nn} = (c_{ij}) = \sigma_o^2 \exp(-\rho|i-j|)$ , i.e.  $\rho$  is the correlation between adjacent noise elements. Then we can compare the variance  $\hat{\sigma}_{x1}^2$  estimated from a correlation with white noise ( $C = \sigma_o^2 I$ ) and the variance  $\hat{\sigma}_{x2}^2$  from a correlation with coloured noise, especially  $C = C_{nn}$ . The ratio  $V$  of the expected values of the variances then can be obtained from (the derivation is a bit tedious)

$$V = \frac{E(\hat{\sigma}_{x2}^2 | C = C_{nn})}{E(\hat{\sigma}_{x1}^2 | C = \sigma_o^2 I)} = \lambda \frac{n-\lambda}{n-1} \quad (18)$$

where  $\lambda(g_x) = g_x' C^{-1} C_{nn} C^{-1} g_x / g_x' C^{-1} g_x$  in the case  $C = \sigma_o^2 I$  lies within the range of the extreme eigenvalues  $\lambda_{min} = (1-\rho)/(1+\rho)$  and  $\lambda_{max} = (1+\rho)/(1-\rho)$  of the Toeplitz matrix  $C_{nn}$  for the number of pixels being large ( $n \rightarrow \infty$ , cf. Grenander and Szegö 1958). The first term in eq. (18) results from the error in the normal equations; it is dominant to the second term  $(n-\lambda)/(n-1)$  resulting from the error in the estimation of the noise variance. Taking  $\rho = 0.8$ , a value which has been proved to be realistic for multitemporal images (cf. Svedlov et. al. 1976), results in  $1/9 < \lambda < 9$ . This means that the standard deviation for the shift estimated from a least squares adjustment using the wrong covariance matrix  $C = \sigma_o^2 I$  might be wrong up to a factor 3 in both directions. The standard deviation will be too optimistic if  $g_x$ , the derivative of the signal, is long waved, i.e. without high frequencies. The estimated shift, however, is nearly not influenced by using a slightly wrong covariance matrix, especially it still is an unbiased estimator (cf. Koch 1980, p. 164).

2. The effect of nonlinear filters usually is difficult to predict. The statistical properties of the median filter, though, especially with respect to contaminated edge images have been extensively investigated by Justusson (1981). His results can be used to predict the effect of the median filter on the restoration of the gradient which is necessary for point transfer (cf. sect. 2.3.1) when applying the iterative least squares approach (eq. (10)), where  $g_{x,i}$  and  $g_{y,i}$  have to be estimated from one of the two images.

If one keeps the effect of a linear and a nonlinear filter onto the variance  $\sigma_{nx}^2$  of the gradient of the noise constant one is able to compare their effect on the variance  $\sigma_{gx}^2$  of the signal gradient  $g_x$  and with eq. (13) onto the precision of the template matching. Geiselmann investigated the gain in precision based on the theoretical results by Justusson and on computer simulations (cf. Geiselmann 1983). Using the conventional way of calculation the gradient  $(g_{i+1} - g_{i-1})/2$  the standard deviation  $\sigma_x$  is smaller by a factor 1.35 if the median with 3 or 3x3 pixels is used for restoration. If however the sharper gradient  $g_{i+1} - g_{i-1}$  is used the gain in precision is a factor 1.6, showing the smoothing effect of the conventional gradient computation. Moreover, if the median with 5 or 5x5 pixels is applied the gain is larger than a factor 2. It depends on the ratio of the height of the edge and the standard deviation of the noise. The gain is even higher, about 20 % if the noise has a longtailed, e.g. a Student distribution. The findings are in full agreement with those from Yang and Huang (1981). They also showed that the effect of the median filter is greatly reduced if the edge is not sharp but a ramp.

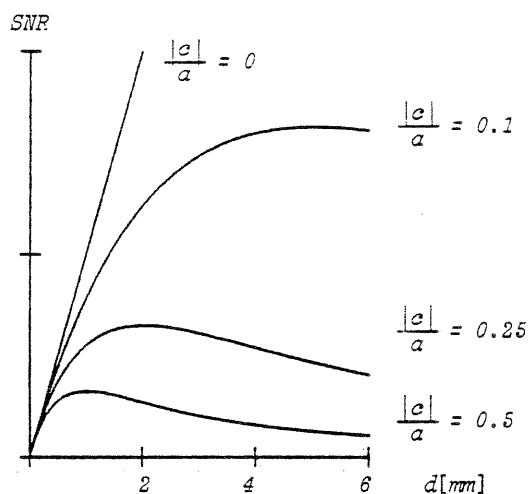
### 3.4 The sensitivity of the matched filter

The effect of unmodelled geometric distortions in the correlation may cause systematic effects and reduce the total accuracy of the match. Specifically, we will investigate the influence of scale differences between the two images in concern.

1. In the presence of geometric distortions there exists an optimal patch size for correlation (cf. Svedlov et.al. 1976) as small patches do not contain enough pixels and large patches cannot

be matched well because of the geometric distortions. Fig. 5 shows the influence of scale errors onto the output signal to noise ratio. These theoretical results are adapted from Svedlow et.al. (1976). They are based on the AR-image model with white noise perturbation. The results here are given in dependency on the parameter  $\alpha$ , with  $\alpha = 5r$  (cf. sect. 3.1). Clearly the effect of scale

Fig. 5  
Output signal to noise ratio for different values of scale distortion  $c$  versus the length  $d$  of a square area (adapted from Svedlow et.al. 1976). with autocovariance function  $R = R_0 e^{-|x|/r}$ , and  $\alpha = 5r$



distortion will increase with increasing scale difference and decrease with increasing correlation length  $r$ , thus increasing  $\alpha$ , as the image is smoother for large  $\alpha$ . The optimum patch size  $d_{opt} \times d_{opt}$  with  $d_{opt} = 2.5r / |c|$  proves to be

$$d_{opt} = 0.5 \frac{\alpha}{|c|} \quad (19)$$

For good imagery and a scale difference of 0.1 the optimum size is 1 mm<sup>2</sup>. Fig. 5 shows that for smaller patches the increase of the signal to noise ratio is approximately proportional to the patch side  $d$ . Svedlov et. al. also analysed the effect of unmodelled rotation differences and more general deformations occurring in LANDSAT images. As for high precision correlation at least linear geometric deformations should be compensated by the algorithm it would be worth to investigate the influence of unmodelled nonlinear distortions representing the local curvature of the terrain. As the effective bandwidth of the image is not much influenced by geometric distortions eq. (13) also holds for the minimum variance  $\sigma_w^2$ .

Actually very small patch sizes of only 5x5 pels are used in TV image sequence analysis (cf. Dinse et.al. 1981, Bergmann 1982). In photogrammetric applications the patch size varies between 11x11 pels (cf. v. Roessel 1972, Gambino and Crombie 1974) and 32x32 pels (e.g. Markarian et.al. 1973). Hence most systems do not seem to take full advantage of the accuracy potential. Obviously severe local nonlinearities, especially occurring in large scales, require to use smaller correlation windows, accepting the decrease in accuracy.

2. Quite a different approach to compensate for unknown scale differences or other geometric distortions is to look for a point  $C(x_s, y_s)$  within the patch whose transformed point  $C'(T_g(x_s, y_s))$  is invariant to scale differences between the images. Thus the bias  $C' - \tilde{C}'_1$  is eliminated. It can be shown for one-dimensional signals that this point is the weighted centre of gravity of the patch, where the weights are the squares of the gradient

$$x_s = \frac{\sum w_i g_{x,i}^2}{\sum g_{x,i}^2} \quad (20)$$

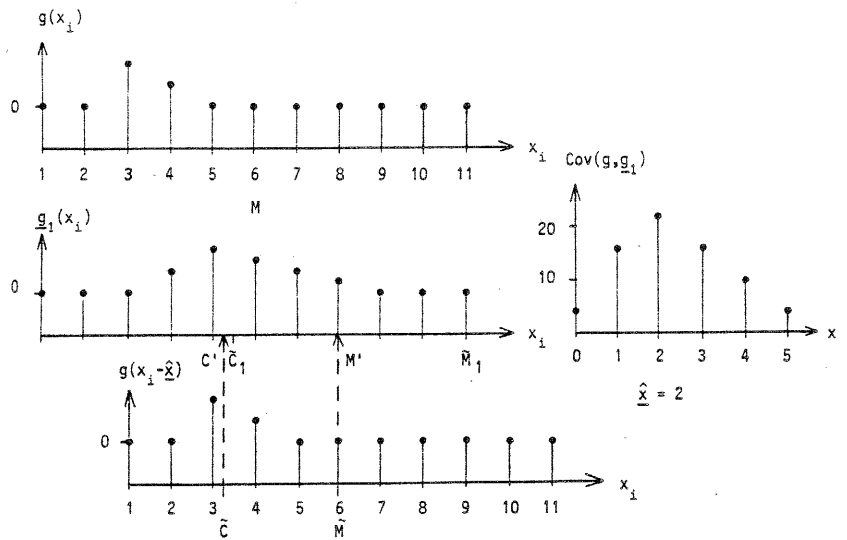
The proof uses the fact that additional parameters in a least squares problem do not influence the result if they are orthogonal to the other unknowns (cf. Förstner 1982). As the partial de-



derivatives of the function  $g(x)$  with respect to shift and scale are  $g_{x,i}$  and  $g_{x,i} \cdot (x_i - x_0)$  resp., where  $x_0$  is the origin of the coordinate system (usually  $x_0 = 0$  is chosen), this leads to the condition  $\sum g_{x,i}^2 (x_i - x_0) = 0$ , from which eq. (20) is derived.

Fig. 6

On the optimal choice of the transferred point when a scale difference is present.  $\tilde{C}$  and  $\tilde{C}_1$  = weighted centres of gravity.  $\tilde{M}$  = middle of template  $g$ . Transferred points  $C'$  and  $M'$ : error  $M' - \tilde{M}_1 = 3$ , error  $C' - \tilde{C}_1 = 0.2$



An example is given in fig. 6. The object  $g(x_i)$  and the signal  $g_1(x_i)$  differ by a scale difference. The covariance function leads to a shift of  $\hat{x} = 2$ . If the centre  $\tilde{M}$  of the template is transferred, i. e. shifted by 2, the bias  $M' - \tilde{M}_1 = 3$  is very large. But if one transfers the centre  $\tilde{C}$  of gravity one obtains the point  $C'$  which is very close to the true centre  $\tilde{C}_1$  of gravity. The bias of 0.2 is due to discretization errors.

The centre of gravity is not optimum in two-dimensional patches, but clearly reduces the effect of unmodelled geometric distortions.

### 3.5 Convergence and pull-in-range

The convergence and the pull-in-range are essential for the economy of the least squares procedure. Especially the requirements for the approximate values are determined by the pull-in-range. We will analyse the pull-in-range for the case where no noise is present. Again we restrict the discussion to one-dimensional signals.

The shift is estimated from the maximum of the cross correlation function  $R_{gg_1}(x)$  which for the noiseless case reduces to the autocovariance function  $R_g(x)$ . Suppose the signal is ideal band limited resulting from sampling with pixel size  $\Delta x$  and assuming the signal to be white. Then  $R_g(x) = R_0 \text{ si } \pi x / \Delta x$ . The least squares algorithm eq. (11b) is equivalent to a Newton-Raphson approach to search for the maximum, adapting the gradient to the actual approximate values. The gradient technique, where the gradient is kept constant, and the Newton-Raphson iteration scheme for this application have been excellently discussed by Burkhardt and Moll (1978).

They showed that the convergence rate is cubic. This is due to the symmetry of the autocovariance function at the maximum. In general the Newton-Raphson iteration scheme only reaches quadratic convergence.

Moreover they proved that the pull-in-range is rather small compared to the gradient technique. Thus the approximate values must fulfill the condition  $|x_0| < 1.52 / \pi \cdot \Delta x = 0.48 \Delta x$ , thus must be better than half a pixel. However, though the actual position of the object is not known the gradient of  $R_{x,g}(0)$ , i.e. the curvature of  $R_g(0)$  at the maximum is known. Burkhardt and Moll showed that it can be used to increase the pull-in-range of the Newton-Raphson approach by nearly a factor 3. The approximate values then only have to be accurate up to 1.5 pixels. This result can be used also in multiparameter estimation with the least squares approach, as usually good approxi-

mate values for the additional parameters are available. The idea then is to keep the normal equation matrix constant and only vary the right sides  $h$ . This would also lead to an increase of speed and would quite well fit into a robust algorithm with modified residuals (cf. also Meyers and Frank 1980).

The condition  $|\omega_0| < 1.5 \Delta\omega$  can be used in the form  $\omega_0 < 3/4 \omega_0$ , thus yielding an upper bound for the boundary frequency of a low pass filter which guarantees convergence if the approximate value is supposed to be inaccurate up to  $\omega_0$ .

The discussion of the different quality measures up to now was more or less based on the same mathematical model for the correlation algorithm and the image. The equivalence of the matched filter and the least squares approach could be used to advantage. The following results are based on computer simulations alone, as especially the determination of the reliability would require the derivation of the joint probability density function of the estimated cross covariance function involving the fourth moments of the original signal. The results however prove to be essential for assessing the quality of digital correlation procedures.

### 3.6 The reliability of digital point transfer

As already pointed out in sect. 2 the matched filter may lead to quite wrong results. This is due to the small pull-in-range but even more to the existence of relative maxima of the cross correlation function which in case of disturbances might become the absolute maximum. The aim is to decrease the number of false matches which can be done by trying to increase the probability of correct matches, i.e. the reliability. The proposed filters  $m_2$ ,  $m_3$  and  $m_4$  prove to be appropriate for this purpose.

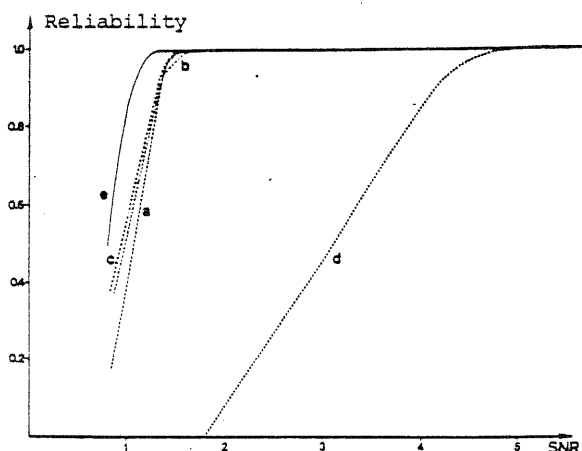
The results of a thorough investigation by Ehlers (1982) are shown in fig. 7a and b. He compared 5 different filters for point transfer with respect to their robustness against additional noise.

These were :

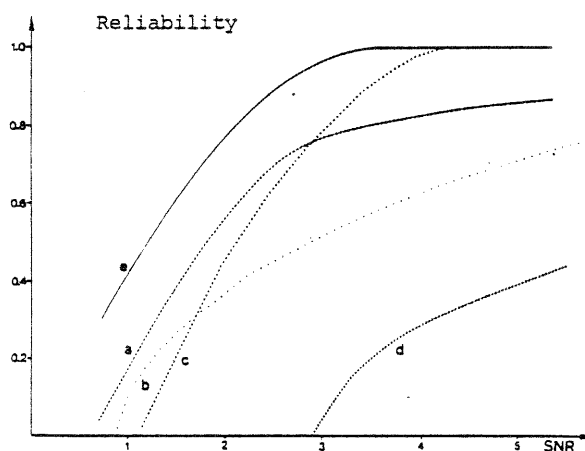
- a. cross correlation
- b. complex exponentiation with local variance
- c. complex exponentiation with global variance
- d. least sum
- e. phase correlation.

Fig. 7 Reliability of point transfer using different filters. Probability of a correct match vs. the SNR, used filters cf. text above (from Ehlers 1982) patch sizes 30x30 and 11x11

a. points with high contrast



b. points with low contrast



The simulation was based on 20 points with low and 20 points with high contrast, selected from one image which was taken as true object and contaminated by Gaussian noise of different variance. The signal to noise ratio varied between 0.8 and 20. The result of a match was accepted if the estimated shift was 1 pixel or less giving an estimate for the reliability of the procedures in dependency of the *SNR*.

- The results for points with high and low contrast demonstrate the influence of the texture of the object, namely the gradient  $g_x$ . The highest reliability in both cases is reached with the phase correlation (e.). For good points the *SNR* might even be below 1, still yielding a reliability of 0.8 or better. The dominance of the phase correlation, being representative for whitening filters becomes clear from fig. 7b for the points with low contrast. The worst reliability is (d.) obtained with the least sum method, which should be robust against noise. The reason for this behavior is not quite clear, it might be caused by the type of distribution of the noise. The complex exponentiation (b.) with local adaption to the variance proves to be as reliable as cross-correlation (a.). For small signal to noise ratios however there is a slight difference in favour of the complex exponentiation.

The investigation clearly demonstrates that for low signal to noise ratios the reliability of correlation can be increased significantly by sharpening the peak of the correlation function.

### 3.7 The effect of quantization and data compression

Multi-image correlation as discussed in sect. 2.3 requires the storage of a large number of image patches. In order to reduce the necessary storage the data have to be compressed. A pure redundancy reduction where the original image can be restored without loss is not efficient enough. But information reduction will cause quantization errors and thus increase the noise component in the images. Consequently the reliability and the precision will be worse.

1. Table 5 is taken from Bailey et.al. (1976) and shows the effect of *quantization* on the *reliability* for 5 different scenes using 25 points in each scene. The data are digitized pictures. The reliability values are given for the median absolute deviation (MAD) and the normal product covariance (NProd). 4 different quantization levels are investigated. The patch sizes of  $g_1$  and  $g_2$  were 20x20 and 5x5 resp..

Table 5 Effect of Quantization on the probability of Correlation  
(from Bailey et. al. 1976)

Scene Type	Quantization Scheme							
	Continuous		8-level		4-level		Binary	
	MAD	NProd	MAD	NProd	MAD	NProd	MAD	NProd
Random	.90	.95	.78	.87	.65	.74	.30	.30
Agricultural	.72	.72	.64	.52	.36	.40	.36	.36
Mountains	.76	.72	.60	.60	.36	.32	.28	.28
Desert	.92	.92	.80	.80	.48	.56	.36	.36
Suburban	.80	.92	.72	.80	.68	.72	.36	.36

Obviously the reliability decreases monotonically with decreasing quantization level. A quantization with only 4 levels on an average seems to be not sufficient. Also the MAD clearly gives worse results than the covariance (NProd), which does not quite follow the expectations, as the MAD is a robust measure. The results are based on unmodified data, where not all 64 grey levels are present in some of the regions. This should be kept in mind when analysing the results.

2. Table 6 is taken from Mikhail et. al. (1983) and shows the effect of *data compression* onto the *precision* of object location for 24 artificial cross targets introduced into digitized imagery. The precision of the location is estimated from the results of a least squares approach.

Table 6 Empirical precision of target location vs. data compression rate, standard deviations in pels (adapted from Mikhail 1983)

	8 bit/pel	2 bit/pel	1 bit/pel	0.5 bit/pel
noiseless	0.028	0.054	0.105	0.28
with noise	0.038	0.058	0.115	0.53

The precision is determined for the case where additional noise is introduced, having 1/4 of the standard deviation of the signal background and for the noiseless case. The original data being quantized to 8 bit/pel have been compressed to 2, 1 and 0.5 bit/pel using the cosine transform compression method.

The results clearly show the decrease in precision due to information reduction. The additional noise seems to have an influence on the precision in the extrem cases. Data compression down to 0.5 bit/pel seems to cause problems, as the identification process of the procedure (using the Fourier descriptors) is not able to work when one leg of a cross target is missing. The identification using the moments of the patch however worked also in these cases. Nevertheless, even when data are compressed to 1 bit/pel the precision of target location is still 1/10 of a pixel.

Both investigations give clear indication that data compression decreases the quality of correlation. Further research has to clarify whether there are methods to economically store templates without losing too much information needed for high precision image correlation.

The previous sections discussed quality measures which have a direct impact on the economy of the whole procedure of image correlation. Of course there are other aspects which strongly influence the performance, e.g. hierarchical structures (cf. Sharp 1965, Pearson et. al. 1977, Hobrough 1978, Tanaka 1978, Wong 1978, Wong and Hall 1978, Makarovic 1980, Baker 1983) or the use of the epipolar geometry (cf. Helava and Chapelle 1972, Keating 1975, Kreiling 1976, Wrobel 1977, Benard 1982), which could not be treated in this contribution, but on which the relations discussed above might have an influence.

#### 4. Final remarks

Digital image correlation is the basic prerequisite for all tasks in digital photogrammetry and remote sensing where the geometric aspect is dominant. Digital correlation is the bottle neck for an economical implementation of systems for height measurements or differential rectification, but also aerial triangulation, deformation analysis or other high precision applications. The accuracy potential inherent to the images may be used to advantage if the correlation algorithms are able to react on extremely varying situations in an optimal way. This optimum has to be defined by the user who may then apply the results collected in this paper.

Though there are still quite some problems to solve template matching obviously is a simple procedure compared to the algorithms which are necessary for automatic mapping especially in large scales. Here the oversimplification of the mathematical model becomes apparent, as it is only a 2D-model working on the basis of more or less undisturbed images of a smooth surface. Thus digital correlation in its classical form will fail in all cases where the surface to be reconstruct-

ted is not flat anymore. Modifications of the algorithms may efficiently solve some of the problems coming up with images of really 3D-objects. The first examples of the application of pattern recognition principles to photogrammetric problems (cf. Baker 1983, Benard 1983) however show that other concepts are needed which are able to correlate 3D-objects with 3D-models.

## REFERENCES

## Abbreviations:

BuL	Bildmessung und Luftbildwesen
CGIP	Computer Graphics and Image Processing
IAP	International Archives for Photogrammetry
IEEE AES	IEEE Transaction on Aerospace and Electronic Systems
IEEE TC	IEEE Transactions on Computers
IEEE COM	Transactions on Communications
IEEE GE	IEEE Transactions on Geoscience Electronics
IEEE IT	IEEE Transactions on Information Theory
IEEE PAMI	IEEE Transactions on Pattern Analysis and Machine Intelligence
IEEE SMC	IEEE Transactions on Systems Man and Cybernetics
IPS	Schriftenreihe des Instituts für Photogrammetrie Stuttgart
PhEng	Photogrammetric Engineering and Remote Sensing
PhRec	Photogrammetric Record
ZfV	Zeitschrift für Vermessungswesen

- Ackermann F. (1982):* A Concept for Deformation Analysis by Digital Image Processing, in "Fourty Years of Thought", Anniversary Collection for W. Baarda, Delft 1983, pp 36-45
- Ackermann F. (1984):* High Precision Digital Image Correlation, IPS Heft 9, Stuttgart 1984
- Ackermann F., Pertl A. (1983):* Zuordnung kleiner Bildflächen durch digitale Korrelation zur Verknüpfung verschiedener oder verschiedenartiger Bilder im Anwendungsbereich Photogrammetrie und Fernerkundung, DFG-Abschlussbericht, Stuttgart 1983
- Albertz, J., Kreiling W., Wiesel J. (1976):* Weitere Untersuchungen zur Blocktriangulation ohne Punktübertragung. XIIIth ISP Congress, Helsinki 1976, Pres.Paper to Comm. III
- Allan M. (1982):* Limitations of Current Automated Photogrammetric Instrumentation and the Potential of Future Fully Automated Systems. IAP Vo. 24-11, Ottawa 1982, pp. 131-147
- Anuta P.E. (1970):* Spatial Registration of Multi-spectral Digital Imagery Using Fast Fourier Transformation Techniques. IEEE Vol. GE-8, 1970, pp. 353-368
- Bailey H.H., Blackwell F.W., Lowery C.L., Ratkovic H.A. (1976):* Image Correlation, Part I, Simulation and Analysis, Rand Report R-2057/1-PR, 1976
- Baker H.H. (1983):* Surfaces from Mono and Stereo Images, Pres. Paper, Specialist Workshop on Pattern Recognition in Photogr., Graz 1983
- Barnea D.T., Silverman H.F. (1972):* A Class of Algorithmus for Fast Digital Image Registration, IEEE Vol. TC-21, 1972, p. 179-186
- Benard M. (1983):* Automatic Stereophotogrammetry: A Method Based on Feature Detection and Dynamic Programming, Pres. Paper, Specialist Workshop on Pattern Recognition in Photogrammetry, Graz 1983
- Bergmann H.C. (1982):* Displacement Estimation Based on the Correlation of Image Segments, Int. Conf. on Electronic Image Processing, 1982
- Bernstein R. (1973):* Scene Correction (Precision Processing) of ERTS Sensor Data Using Digital Image Processing Techniques. 3rd ERTS Symp., Vol. 1-A, NASA SP-351, 1973
- Bernstein R., Ferneyhough D.G. (1975):* Digital Image Processing, PhEng Vol. 41, 1975, pp. 1465-1476
- Bernstein R. (1983):* Image Geometry and Rectification, Manual of Remote Sensing, Second Edition, Ch 21, ASP, Little Falls Church 1983
- Billingsley F.C. (1982):* Interim Report of Working Group 11/3, Instruments for Analysis of Remotely Sensed Data, IAP Vo. 24-11, Ottawa 1982, pp. 215-224
- Burkhardt H., Moll H. (1979):* A Modified Newton-Raphson Search for the Model-Adaptive Identification of Delays, 5. IFAC-Symposium on Identification and System Parameter Estimation, Darmstadt 1979, pp. 1279-1286
- Cafforio C., Rocca F. (1976):* Methods for Measuring Small Displacements of Television Images, IEEE Vol. IT-22, pp. 573-579
- Cafforio C., Rocca F. (1979):* Tracking Moving Objects in Television Images, Signal Processing 1
- Casasent D., Psaltis D. (1975):* Position, Rotation and Scale Invariant Optical Correlation, Applied Optics Vol. 15-7, pp. 1795-1799
- Case J.B. (1980):* Automation in Photogrammetrie, IAP Vol. 23-B2, Hamburg 1980, p. 38-49
- Castleman K.R. (1979):* Digital Image Processing, Prentice Hall, N.J., 1979
- Claus M. (1983):* Digital Terrain Models Through Digital Stereo Correlation. Pres. Paper, Specialist Workshop on Pattern Recognition in Photogrammetry, Graz 1983
- Davis L. S. (1975):* A Survey on Edge Detection Techniques, CGIP Vol. 4, 1975, pp. 248-270
- Dinse Th., Enkelmann W., Nagel H.H. (1981):* Untersuchungen von Verschiebungsvektorfeldern in Bildfolgen, Informatik Fachberichte 49, Heidelberg 1981, pp. 59-75
- Downman I.J., Haggag A. (1977):* Digital Image Correlation Along Epipolar Lines. Mitteilungen der Geod. Inst. d. TU Graz, 29/1977, pp 47-49
- Downman I.J. (1982):* The Performance of Correlation Systems. IAP Vol. 24-11, Ottawa 1982, pp. 172-181
- Dubois B., Prasada B., Sabri M.S. (1981):* Image Sequence Coding, in: Huang (1981): Image Sequence Analysis,
- Ehlers M. (1982):* Increase in Correlation Accuracy of Remote Sensing Imagery by Digital Filtering, PhEng Vol. 48-3, 1982, pp.415-420
- Ehlers M. (1982):* Digital Image Processing of Remote Sensing Imagery: A Comparative Study on Different Object Functions in Correlation Process. Symp. ISP Comm. VII, Toulouse 1982

- Ehlers M. (1983): Untersuchung von digitalen Korrelationsverfahren zur Entzerrung von Fernerkundungsaufnahmen. Wiss. Arb. der Fachr. Verm. wesen d. Univ. Hannover, Nr. 121, 1983
- Emmert R.A., McGillem C.D. (1973): Conjugate Point Determination for Multitemporal Overlay, LARS 1973, Inf. Note 111872
- Fennema C.L., Thompson W.B. (1979): Velocity Determination in Scenes Containing Several Moving Objects, DGIP Vol. 9, 1979, pp 301-315
- Förstner W. (1982): On the Geometric Precision of Digital Correlation, IAP Vol. 24-III, Helsinki 1982, pp. 176-189
- Förstner W. (1982): Systematic Errors in Photogrammetric Point Determination, Meeting of FIG Study Group Vb, Aalborg, Schriftenr. der HSBW, München 1982,
- Förstner W., Klein H. (1984): Realization of Automatic Error Detection in the Block-Adjustment Program PAT-M Using Robust Estimators, IAP Vol. 25-III, Rio de Janeiro 1984
- Gambino L.A., Crombie M.A. (1974): Digital Mapping and Digital Image Processing, PhEng 1974, pp. 1295-1302
- Geiselmann C. (1983): Theoretische Untersuchungen zur Genauigkeitssteigerung der Digitalen Bildkorrelation durch Medianfilterung, Selbst. Arbeit am Inst. f. Photogrammetrie Stuttgart, 1983
- Grenander U., Szegö G. (1958): Teopltitz Forms and Their Applications, University of California Press, Berkeley 1958,
- Göpfert W. (1977): Digital Cross-Correlation of Complex Exponentiated Inputs, Mitteilungen d. Geod. Inst. d. TU Graz, 29/1977, pp. 63-66
- Göpfert w. (1978): Digitale Korrelation komplex exponierter Daten, ZFV 10/1978, pp. 475-484
- Götze G. (1983): Robust Statistical Methods, DGK A 98, München 1983 ,pp. 23-28
- Hall E.L., Davies D.L., Casey M.E. (1980): The Selection of Critical Subsets for Signal, Image and Scene Matching. IEEE Vol. PAMI-2, 1980, pp. 313-322
- Helava U.V., Chapelle W.E. (1972): Epipolar-Scan Correlation, Bendix Technical Journal, Vol. 5, 1972, pp. 19-23
- Helava U.V. (1976): Digital Correlation in Photogrammetric Instruments. IAP Vol. 23-II, Helsinki 1976
- Hill J.W. (1983): Dimensional Measurement for Quantized Images. SRI Project 4391, 1980, in: Ho 1983
- Ho C.S. (1983): Precision of Digital Vision Systems. IEEE Vol. PAMI-5, 1983
- Hobrough G.L. (1959): Automatic Stereo Plotting, PhEng 25-5, 1959, pp. 763-769
- Hobrough G.L., Hobrough T.B. (1971) Image Correlation Speed Limits, BuL 1/1971, pp. 20-24
- Hobrough G. (1978): Digital On-Line Correlation, BuL 3/1978, pp. 79-86
- Huang T.S. (Ed.) (1981): Image Sequence Analysis, Springer New York, 1981
- Huang, T.S., Hsu, .P. (1981): Image Sequence Enhancement, in: Huang (1981): Image Sequence Analysis,
- Huang T.S., Tsai R.Y. (1981): Image Sequence Analysis, in: Huang (1981): Image Sequence Analysis,
- Huber P.J. (1981): Robust Statistics, New York 1981
- Inigo R.M., McVey E. (1981): CCD Implementation of a Three-Dimensional Video Tracking Algorithm, IEEE Vol. PAMI-3, 1981, pp. 230-240
- Justusson B.I. (1981): Median Filters: Statistical Properties, in "Twodimensional Digital Signal Processing II", ed. by Huang T.S., Topics in Appl. Physics 43, Springer, 1981
- Keating T.J., Wolf P.R., Scarpace F.L. (1975): An Improved Method of Digital Image Correlation, PhEng Vol. 41, 1975, pp. 993-1002
- Klaasman H. (1975): Some Aspects on the Accuracy of the Approximated Position of a Straight Line on a Square Grid. CGIP Vol. 4, 1975
- Koch, K.R. (1980): Parameterschätzung und Hypothesentests in Linearen Modellen, Dümmler 1980
- Konecny G. (1977): Digitale Prozessoren für Entzerrung und Bildkorrelation, Schriftenr. d. Inst. f. Photogr. Hannover, Heft 2/1977,
- Konecny G., Pape D. (1981): Correlation Techniques and Devices, PhEng, 47/4, pp 323-333
- Krarup T., Juhl J., Kubik K. (1980): Götterdämmerung over Least Squares, IAP Vol. 23-B3, Hamburg 1980, pp. 369-378
- Kreiling W. (1976): Automatische Auswertung von Stereobildern durch digitale Korrelation, IAP 23, Helsinki 1976
- Kubik K. (1984): Gross Data Errors and Robust Estimation, IAP Vol. 24-III, Rio de Janeiro 1984
- Kuglin C.D., Hines D.C. (1975): The Phase Correlation Image Alignment Method. Proc. of the IEEE Int. Conf. on Cybernetics and Society, 1975. pp. 163-165
- Kuznetsov V.P. (1976): Stable Detection when the Signal and Spectrum of Normal Noise are inaccurately known. Telecommunication Radio Engineering, Vo. 30/31, 1976, pp. 58-64
- Lichtenegger J., Seidel K. (1978): Methoden zur Überlagerung von LANDSAT-Bildern für multitemporale Landnutzungskartierungen, BuL 2/1978, pp. 53-61
- Limb J.O., Murphy J.A. (1975): Measuring the Speed of Moving Objects from Television Signals, IEEE Vol. COM-23, 1975, pp. 474-478
- Lindlohr W. (1981): Untersuchungen zur Varianzkomponentenschätzung bei der Interpolation von Geländeprofilen, Diplomarbeit, Inst.f. Photogr., Stuttgart 1981
- Lugnani J.B. (1982): The Digitized Features - A New Source Control, Pres. Paper, ISP Comm. III Symposium, Helsinki 1981
- Makarovic B. (1980): Automatic Off-Line Generation of Digital Terrain Models, IAP 23-B2, Hamburg 1980, pp. 167-176
- Makarovic B. (1980): Image Correlation Algorithms, IAP 23-B2, Hamburg 1980, pp. 139-158
- Marckwardt W. (1982): Mathematical Models for the Automation of Differential Rectification, IAP Vol. 24-III, Helsinki 1982, pp. 343-353
- Markarian H., Bernstein R., Ferneyhough D.G., Sharp F.S. (1973): Digital Correction for High Resolution Images, Journal Americ. Soc. of Photogramm., Vol. 49/1973, pp. 1311-1320
- Martin R.D., McGath C.P. (1984): Robust Detection of Stochastic Signals, IEEE Vol. IT-20, 1974, pp. 537-541
- Masry S.E. (1981): Digital Mapping Using Entities: A new Concept. PhEng Vol. 48, 1981, pp. 1561-1565

- McGillem C.D., M. Svedlow (1976): Image Registration Error Variance as a Measure of Overlay Quality. IEEE Vol. GE-14, 1976, pp.44-49
- McGillem C.D., Svedlow M. (1977): Optimum Filter for Minimizing of Image Registration Error Variance, IEEE Vol. GE-15, 1977 pp.257-259
- Meyers M.H., Franks L.E. (1980): Joint Carrier Phase and Symbol Timing Recovery for PAM Systems, IEEE Vol. COM-28, 1980, pp.1121-1129
- Mikhail M.M. (1983): Photogrammetric Target Location to Subpixel Accuracy in Digital Images, IPS Heft 9, 1984, pp. 217-230
- Mikhail M.M., Akey M.L., Mitchell O.R. (1983): Detection and Sub-Pixel Location of Photogrammetric Targets in Digital Images, Pres. Paper, Specialist Workshop on Pattern Recognition in Photogrammetry, Graz 1983
- Nagel H.H. (1981): Image Sequence Analysis: What can we learn from Applications, in: Huang (1981): Image Sequence Analysis
- Oppenheim A.V., Lim H.S. (1981): The Importance of Phase in Signals, Proceedings of IEEE, Vol. 69, 1981, pp. 529-541
- Panton D.J. (1978): A Flexible Approach to Digital Stereo Mapping, Proc. of the DTM Symposium, ASP, St. Louis 1978, pp.32-60
- Papoulis A. (1965): Probability, Random Variables and Stochastic Processes McGraw Hills, 1965
- Pavlidis Th. (1979): The Use of a Syntactic Shape Analyser for Contour Matching, IEEE Vol. PAMI-1, 1979, pp.307-310
- Pearson J.J., Hine D.C., Golosman S., Kuglin C.D. (1977): Video Rate Image Correlation Processor, SPIE Vol. 119, Application of Digital Image Processing, IOCC 1977, pp.197-205
- Pertl A. (1984): Digital Image Correlation with the Analytical Plotter Planicomp C 100, IAP 25-III, Rio de Janeiro, 1984
- Prabhu K.A., Netravali A.N. (1982): Motion Compensated Component Colour Coding, IEEE Vol. COM-30, 1982, pp. 2519-2527
- Pratt W.K. (1974): Correlation Techniques of Image Registration, IEEE Vol. AES-10, 1974, pp. 353-358
- Rocca F. (1972): TV Bandwidth Compression Utilizing Frame-to-Frame Correlation and Movement Compensation, in: Picture Bandwidth Compression, ed. by T.S. Huang, O.J. Tretiale, London 1972
- Roessel, van J. (1972): Digital Hypsographic Map Compilation, PhEng 38/1972, pp. 1106-1116
- Roos M. (1975): The Automatic Reseau Measuring Equipment (ARME), PhEng 41/1975, pp.1109-1115
- Rosenfeld A., Kak A.C. (1976): Digital Picture Processing, Acad. Press, New York 1976
- Ryan T.W., Gray R.T., Hunt B.R. (1980): Prediction of Correlation Errors in Stereopair Images, Optical Engineering Vol. 19/1980
- Schalhoff R.J., McVey E.S. (1979): Algorithms Development for Real Time Automatic Video Tracking Systems, Proc. 3rd Int. Computer Software and Application Conf., Chicago, 1979, pp.504-511
- Sharp J.V., Christensen R.L., Gilman W.L., Schulman F.D. (1965): Automatic Map Compilation Using Digital Techniques, PhEng 31/1965, pp. 223-239
- Svedlow M., McGillem C., Anuta P. (1976): Analytical and Experimental Design and Analysis of an Optimal Processor for Image Registration, LARS Inf. Note 090776, Purdue Univ., West Lafayette 1976
- Tanaka M., Tamura S., Tanaka K. (1978): Picture Picture Assembly Using a Hierarchical Partial-Matching Technique. IEEE Vol. SMC-8, 1978, pp.812-819
- Thurgood J.D., Mikhail E.M. (1982): Subpixel Mensuration of Photogrammetric Target in Digital Images. School of Civil Engineering, Purdue CH-PH-82-2
- Thurgood J.D., Mikhail M.M. (1982): Photogrammetric Analysis of Digital Images, IAP Vol. 24-III, pp. 576-590
- Tsuji S., Osada M., Yachid M. (1980): Tracking and Segmentation of Moving Objects in Dynamic Line Images, IEEE Vol. PAMI-2, 1980, pp 516-522
- Urkowitz H. (1953): Filters for Detection of Small Radar Signals in Clutter, J. Applied Physics, Vol. 24, 1953, pp. 1024-1031
- Wallace T.P., Mitchell O.R. (1980): Analysis of Three-Dimensional Movement Using Fourier Descriptors, IEEE Vol. PAMI-2, 1980, pp 583-588
- Wang I.Y.C. (1977): Feature Extraction by Interactive Image Processing, PhEng Vol.43, 1977, pp. 1495-1501
- Werner H. (1984): Automatic Gross Error Detection by Robust Estimators, IAP Vol.25-III, Rio de Janeiro 1984
- Widrow B. (1973): The Rubber Mask Technique-I. Pattern Measurement and Analysis, Pattern Recognition, Vol. 5, 1973, pp.175-198
- Wild E. (1979): Internal Reports, Institut für Photogrammetrie, Stuttgart 1979
- Wiesel W.J. (1981): Paßpunktbestimmung und geometrische Genauigkeit bei der relativen Entzerrung von Abtastdaten, DGK Reihe C-268, München 1981
- Wong R.Y. (1978): Sequential Scene Matching Using Edge Features, IEEE Vol. AES-14, 1978, pp. 128-140
- Wong R., Hall E. (1978): Scene Matching with Invariant Moments, CGIP Vol. 8, 1978, p. 16
- Wong R.Y., Hall E.L. (1979): Performance Comparison of Scene Matching Techniques. IEEE Vol. PAMI-1, 1979, pp. 325-330
- Wrobel B. (1978): Geometrische Aspekte der Korrelationssteuerung, Schriftenr. d. Inst. f. Photogrammetrie Hannover, Heft 2, 1978
- Wrobel B., Ehlers M. (1980): Digitale Korrelation von Fernerkundungsbildern aus Wattgebieten, Bul 48, 1980, pp. 67-79
- Yang G.J., Huang T.S. (1981): The Effect of Median Filtering on Edge Location Estimation. CGIP Vol. 15, 1981, pp. 224-245